Matched coordinates for the analysis of 1D gratings

Gérard Gérard Granet, Joerg Bischoff

Matched coordinates for the analysis of 1D gratings.

Gérard Granet*

Université Clermont Auvergne, CNRS, SIGMA Clermont, Institut Pascal, F-63000 Clermont-Ferrand, France
gerard.granet@uca.fr

Joerg Bischoff

OSIRES Optical Engineering, Schillerstr. 19, D-98693 Ilmenau, Germany (jb@osires.biz)
Joerg.Bischoff@tu-ilmenau.de

April 6, 2021

Abstract

The Fourier modal method (FMM) is certainly one of the most popular and general methods for the modeling of diffraction gratings. However for non-lamellar gratings it is associated with a staircase approximation of the profile leading to poor convergence rate for metallic gratings in TM polarization. One way to overcome the above weakness of the FMM is the use of the fast Fourier factorization (FFF) first derived for the differential method. That approach relies on the definition of normal and tangential vectors to the profile. Instead, we introduce a coordinate system that matches laterally the profile and solve the covariant Maxwell's equations in the new coordinate system, hence the name matched coordinate method (MCM). Comparison of efficiencies computed with MCM with other data from the literature validates the method.

Keywords Computational electromagnetic. 1D Diffraction gratings. Curvilinear coordinates. Pseudo-spectral method. Matched coordinates.

I. Introduction

Nowadays, many methods exist to solve the problem of diffraction by a grating. Among them, differential methods equipped with Fourier series like the RCWA [1], the differential method [2][3] and the C-method [4] [5] are probably the most widespread in that field. Each of them was born in the eighties, has its own area of excellence, and has been greatly improved since the beginnings. In all three methods, both the field components and the coefficients of Maxwell's equation are expanded into Fourier series. These expansions are at the root of most of the problems and limitations of the above methods although the so-called factorization rules are applied. Indeed, it is well known that the convergence of Fourier series is linked with smoothness of the function to be represented. In the C method, the coefficient of Maxwell's equation which is expanded into Fourier series is the derivative of the profile function. Consequently, C-method limitations concern profiles with discontinuous derivatives like echelette gratings, trapezoidal gratings and more generally deep gratings. The remedy is adaptive spatial resolution and parametrization of the profile function [6] [7]. In the RCWA, and the differential method which stay in Cartesian coordinates the coefficients of Maxwell's equations to be Fourier expanded are the permittivity and the permeability functions of the grating. As such, the factorization rules do not take into account the geometry of the grating. In the frame work of the differential method, Popov and Neviere introduced what they called the Fast Fourier Factorization [8]. The factorization rules are implemented after a normal and a tangential vector field has been introduced. In that way, the profile shape is introduced in the algorithm leading to efficient codes. In this paper, following the ideas of C-method, we propose to use matched coordinates to formulate the grating problem. We restrict ourselves to the case where a one dimensional grating is embedded between two planes. Hence the most simple grating is described by two curves separating two different media. The change of coordinates is chosen such that these two curves coincide with coordinates

*Corresponding author

lines, hence the name matched coordinates. Unfortunately, in this formulation, the coefficients of the differential system of Maxwell's equations are not constant which means that the solution in the grating region cannot be obtained thanks to a modal method. Instead, in a manner similar to what was done in [9], we introduce a pseudo-spectral approach to solve the longitudinal dependence of the field along the grooves. In the case of deep gratings the modulated region may be divided into thin enough layers in order to work with smaller matrices. Accurate and fast electromagnetic simulation methods gained considerable importance with the rise of modern technology. Particularly semiconductor manufacturing and metrology play a significant role in pushing the limits. Famous examples are optical scatterometry, a.k.a. as optical CD (OCD) where electromagnetic modeling paved the way for the fast and non-destructive measurement of technical structures in the nano-meter range [10]. However, OCD is just the tip of iceberg. Model based metrology methods are quickly evolving everywhere in dimensional metrology [11]. Other examples are laser focus scanning and white light interferometry [12]. Many technical surfaces either consist of metals or are coated with it. In addition, the profiles are steep or even overhanging. While the RCWA exhibits convergence issues for metallic materials both related to the required stair-case approximation of the profile as well as to the Gibb's phenomenon related to the Fourier expansion, the C-method struggles with multiple materials and very deep profiles. Here, the matched coordinates method may bring relief. We will demonstrate this with some practical examples.

II. Matched coordinates

i. New coordinates

Any method aimed at solving Maxwell's equations works all the more that boundary conditions are properly enforced. Using Matched coordinates helps achieve this requirement. Consider the elementary cell of a planar volume grating as shown in Fig.1. Curves $x = f_1(y)$ and $x = f_2(y)$ separate three domains in which the permittivity is assumed constant with values equal to ϵ_1 and ϵ_2. Now, denoting the period of the grating by d, let us introduce the following change of coordinates from the Cartesian system (x, y, z) to (x^1, x^2, x^3) :

$$\begin{array}{l} x(x^1, x^2) = \\ \left\{ \begin{array}{l} (f_1(x^2) - 0)h_1(x^1) \ \text{ if } \ x^1 \leq u_1 \\ f_1(x^2) + (f_2(x^2) - f_1(x^2))h_2(x^1) \\ \ \text{ if } \ u_1 \leq x^1 < u_2 \\ f_2(x^2) + (d - f_2(x^2))h_3(x^1) \ \text{ if } \ u_2 \leq x^1 < d \end{array} \right. \\ y = x^2 \\ z = x^3 \end{array} \tag{1}$$

$h_1(x^1)$, $h_2(x^1)$, $h_3(x^1)$ should be monotonous increasing functions between 0 and 1. In the new coordinate system, $f_1(y)$ and $f_2(y)$ correspond to coordinate surfaces $x^1 = u_1$ and $x^1 = u_2$ respectively. These surfaces delimit domains in which ϵ is now a function of x^1 alone. We have achieved: $\epsilon(x, y) \rightarrow \epsilon(x^1)$.

$$\epsilon(x^1) = \left\{ \begin{array}{l} \epsilon_1 \ \text{ if } \ x^1 \leq u_1 \\ \epsilon_2 \ \text{ if } \ u_1 \leq x^1 \leq u_2 \\ \epsilon_1 \ \text{ if } \ u_2 \leq x^1 < d \end{array} \right. \tag{2}$$

The choice of $x^1 = u_1$ and $x^1 = u_2$ on the one hand and of functions $h_1(x^1)$, $h_2(x^1)$, $h_3(x^1)$ is quite arbitrary. It determines spatial resolution along x axis. One possible choice is to define the transition points u_1 and u_2 at mid-height of the profile that is:

$$\begin{array}{l} u_1 = f_1(y_m) \\ u_2 = f_2(y_m) \end{array} \tag{3}$$

where y_m is the ordinate at mid-height of the volume grating. In addition, we can also stretch coordinates lines along x in the neighborhood of the transition points as was done in [6], we may take:

$$\begin{array}{l} h_1(x^1) = \dfrac{x^1}{u_1} + \eta \dfrac{x^1_1}{\pi} sin \dfrac{\pi x^1}{u_1} \\ h_2(x^1) = \dfrac{x^1 - u_1}{u_2 - u_1} + \eta \dfrac{x^1 - u_1}{2\pi} sin \dfrac{2\pi(x^1 - u_1)}{u_2 - u_1} \\ h_3(x^1) = \dfrac{x^1 - u_2}{d - u_2} + \eta \dfrac{d - u_2}{\pi} sin \dfrac{\pi(x^1 - u_2)}{d - u_2} \end{array} \tag{4}$$

where η is a parameter between 0 and 1. Please note that input medium and output medium are also affected by the change of coordinate. Indeed, above and below the grating, the x^1 coordinates lines should necessarily coincide with those of the upper face and of the lower face of the grating. They are only Cartesian coordinates with a metric coefficient along x. Above

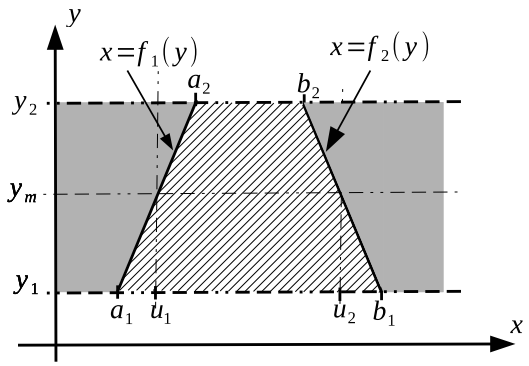

Figure 1: *notation for the new coordinates.* $a_1 = f_1(y_1)$, $a_2 = f_1(y_2)$, $b_1 = f_2(y1)$, $b_2 = f_2(y_2)$, $u_1 = f_1(y_m)$, $u_2 = f_2(y_m)$, $y_m = 0.5(y_1 + y_2)$

the grating $x(x^1, x^2) = x(x^1, x^2 = y_2)$:

$$\begin{array}{l} x(x^1) = a_2 h_1(x^1) \text{ if } x^1 \leq u_1 \\ x(x^1) = a_2 + (b_2 - a_2)h_2(x^1) \text{ if } u_1 < x^1 < u_2 \\ x(x^1) = b_2 + (d - b_2)h_3(x^1) \text{ if } u_2 \leq x^1 \leq d \end{array} \quad (5)$$

and below the grating, $x(x^1, x^2) = x(x^1, x^2 = y_1)$:

$$\begin{array}{l} x(x^1) = a_1 h_1(x^1) \text{ if } x^1 \leq u_1 \\ x(x^1) = a_1 + (b_1 - a_1)h_2(x^1) \text{ if } u_1 < x^1 < u_2 \\ x(x^1) = b_1 + (d - b_1)h_3(x^1) \text{ if } u_2 \leq x^1 \leq d \end{array} \quad (6)$$

where $y = y_2$ and $y = y_1$ are the positions of the upper face and the lower face of the grating layer respectively.

ii. Metric tensor

Denoting $x^i, i = 1, 2, 3$ the new coordinates and $x^{i'}, i' = 1, 2, 3$ the Cartesian coordinates x, y, z, the elements g_{ij} of the fundamental metric tensor are given by:

$$g_{ij} = \frac{\partial x^{i'}(x^i)}{\partial x^i} \frac{\partial x^{j'}(x^j)}{\partial x^j} \delta_{i'j'} \quad (7)$$

$\delta_{i'j'}$ is the Kronecker symbol. However when using Maxwell's equation under the covariant form, the useful quantities are the $\sqrt{g}g^{ij}$ where g is the determinant of g_{ij} and g^{ij} the inverse of the matrix formed by the g_{ij}. Denoting $\frac{\partial x}{\partial x^1}$ by $\partial_1 x$ and $\frac{\partial x}{\partial x^2}$ by $\partial_2 x$, the metric tensor writes:

$$\sqrt{g}\left[g^{ij}\right] = \begin{bmatrix} \frac{1 + (\partial_2 x)^2}{\partial_1 x} & -\partial_2 x & 0 \\ -\partial_2 x & \partial_1 x & 0 \\ 0 & 0 & \partial_1 x \end{bmatrix} \quad (8)$$

In input and output regions, the metric tensor is simplified and reduces to a diagonal since $\partial_2 x$ is null.

iii. 2D Maxwell's equations

Assuming a time dependence of the form $\exp(i\omega t)$,and renormalizing $\mathbf{H}$ by $Z_0\mathbf{H}$ where Z_0 is the vacuum impedance, Maxwell's equation under the covariant form write:

$$\begin{array}{rcl} \xi^{ijk}\partial_j E_k &=& -ik\mu^{ij}H_j, \\ \xi^{ijk}\partial_j H_k &=& +ik\epsilon^{ij}E_j, \quad 1 \leq i, j \leq 3. \end{array} \quad (9)$$

where:

- the ϵ^{ij} and μ^{ij} are given by:

$$\begin{array}{l} \epsilon^{ij}(x^1, x^2) = \epsilon(x^1)\sqrt{g(x^1, x^2)}g^{ij}(x^1, x^2) \\ \mu^{ij}(x^1, x^2) = \sqrt{g(x^1, x^2)}g^{ij}(x^1, x^2) \end{array} \quad (10)$$

- ξ^{ijk} is the Levi-Civita indicator whose the only non-zero elements are: $\xi^{123} = \xi^{231} = \xi^{312} = 1, \quad \xi^{132} = \xi^{213} = \xi^{321} = -1.$
- ∂_i represent the partial derivative $(\partial/\partial x^i)$ versus x^i
- g is the determinant of the fundamental metric tensor

The constitutive relations are such that ϵ^{i3} and μ^{i3} are null. In the case of classical incidence, the general system of differential equations 9 separates into two independent subsystems corresponding to TM and TE polarisations. We get:

$$\partial_2 \begin{bmatrix} \mathcal{F} \\ \mathcal{G} \end{bmatrix} = \begin{bmatrix} -\frac{\chi^{12}}{\chi^{22}}\partial_1 & -ik\left(\chi^{11} - \chi^{12}\frac{1}{\chi^{22}}\chi^{21}\right) \\ ik\chi^{33} - \frac{i}{k}\partial_1\frac{1}{\chi^{22}}\partial_1 & -\partial_1\frac{\chi^{21}}{\chi^{22}} \end{bmatrix} \begin{bmatrix} \mathcal{F} \\ \mathcal{G} \end{bmatrix} \quad (11)$$

with :

$$\begin{bmatrix} \mathcal{F} \\ \mathcal{G} \end{bmatrix} = \begin{cases} \begin{bmatrix} H_3 \\ E_1 \end{bmatrix} \text{ for TM polarization} \\ \begin{bmatrix} E_3 \\ H_1 \end{bmatrix} \text{ for TE polarization} \end{cases} \quad (12)$$

and

$$\begin{bmatrix} \chi^{11} & \chi^{12} & 0 \\ \chi^{21} & \chi^{22} & 0 \\ 0 & 0 & \chi^{33} \end{bmatrix} = \begin{cases} \begin{bmatrix} -\epsilon^{11} & -\epsilon^{12} & 0 \\ -\epsilon^{21} & -\epsilon^{22} & 0 \\ 0 & 0 & \mu^{33} \end{bmatrix} \text{ for TM polarization} \\ \begin{bmatrix} \mu^{11} & \mu^{12} & 0 \\ \mu^{21} & \mu^{22} & 0 \\ 0 & 0 & -\epsilon^{33} \end{bmatrix} \text{ for TE polarization} \end{cases} \tag{13}$$

In homogeneous regions 1 and 3, the TE and TM solution can be obtained from the same scalar propagation equation:

$$\left(\partial_2^2 + \frac{1}{\sqrt{g}}\partial_1 \frac{1}{\sqrt{g}}\partial_1 + k^2\epsilon\right)\mathcal{F} = 0 \tag{14}$$

It has to be noted that the metric factor $\sqrt{g}$ is different in region 1 and region 3. Matching the field at surfaces $x^2 =$ constant requires the knowledge of $\mathcal{G}$ which is deduced from $\mathcal{F}$ by:

$$\mathcal{G} = \begin{cases} = \frac{-i}{k}\frac{\sqrt{g}}{\epsilon}\partial_2\mathcal{F} \text{ for TM polarization} \\ = \frac{i}{k}\sqrt{g}\partial_2\mathcal{F} \text{ for TE polarization} \end{cases} \tag{15}$$

III. Method of Solution

In this section, we give the lines which lead to the solution of the problem using matched coordinates. From the physicist's view point, the grating problem consists of some grating region embedded between two homogeneous media and enlightened from one side by a plane wave. The problem is to calculate the complex amplitude and the phase of the outgoing waves from the grating and then the reflected and eventually transmitted diffracted orders. We have seen that for the one-dimensional case Maxwell's equations reduce to:

$$\partial_2 \begin{bmatrix} F(x^1,x^2) \\ G(x^1,x^2) \end{bmatrix} = \mathcal{L}(x^1,x^2) \begin{bmatrix} F(x^1,x^2) \\ G(x^1,x^2) \end{bmatrix} \tag{16}$$

In the input and output regions, the operator $\mathcal{L}$ is particular in that it does not depend on x^2. So we will derive the solution separately in the input and output regions and in the grating region itself. However, regarding the x^1 dependence, in every region, we may expand the field onto the same basis U_m and write:

$$\begin{aligned} \mathcal{F}_p(x^1,x^2) &= \textstyle\sum_m F_{p\,m} U_m(x^1) V_p(x^2) \\ \mathcal{G}_p(x^1,x^2) &= \textstyle\sum_m G_{p\,m} U_m(x^1) V_p(x^2) \end{aligned} \tag{17}$$

where the subscript letter p refers to the region. At this stage, $U_m(x^1)$ may be quite arbitrary. In particular, it could be a sub-domain basis as those who were implemented for the modal analysis of lamellar gratings. However in this paper we will restrict ourselves to U_m being pseudo-periodic functions:

$$U_m(x^1) = \exp\left(-ik\alpha_m x^1\right) \tag{18}$$

with

$$\alpha_m = \alpha_0 + m\frac{\lambda}{d} \tag{19}$$

where α_0 is the pseudo periodic coefficient. When the incident wave vector is inclined at an angle θ with respect to the vertical axis, $\alpha_0 = n\sin(\theta)$ with n the optical index of the input medium. In the next paragraphs, we derive the solution in homogeneous regions and in the grating region respectively.

i. In homogeneous regions

In input and out regions, since the operator $\mathcal{L}$ is independent of x^2 we have solutions of the form:

$$\mathcal{F}(x^1,x^2) = \sum_q A_q^{\pm} \exp(\mp i\beta_q x^2) F_q^{\pm}(x^1) \tag{20}$$

where $F_q^{\pm}(x^1)$ and β_q are respectively an eigen vector and an eigen value of the eigen equation deduced from Eq(14):

$$\beta_q^2 F_q^{\pm}(x^1) = \left(\frac{1}{\sqrt{g}}\partial_1\frac{1}{\sqrt{g}}\partial_1 + k^2\epsilon\right)F_q^{\pm}(x^1) \tag{21}$$

The exponents $+$ and $-$ refer to forward and backward waves respectively. The eigenvalues β_q are obtained from their square number and are the same for both polarisations:

$$\beta_q = \begin{cases} \sqrt{\beta_q^2} & \text{if } \epsilon \text{ is real and } \beta_q^2 \geq 0 \\ -i\sqrt{\beta_q^2} & \text{if } \epsilon \text{ is real and } \beta_q^2 \leq 0 \\ \sqrt{\beta_q^2} & \Im(\beta_q) < 0 \text{ if } \epsilon \text{ is complex} \end{cases} \tag{22}$$

Of course a similar expression holds for $\mathcal{G}$. Please note that $F^+(x^1) = F^-(x^1)$. We have introduced the superscript $\pm$ to emphasize that we have forward and backward waves. In Fourier space, the partial derivative ∂_1

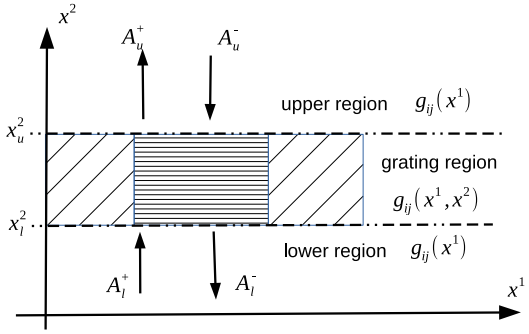

Figure 2: *Illustration of the partition of the problem in three regions. We only have modal expansions in the upper and lower regions.*

is associated to the diagonal matrix formed by the α_m and $1/\sqrt{g}$ is associated to the inverse of the toeplitz matrix built with the Fourier coefficients of the derivative of $x(x^1)$. The details of the derivation may be found in [6]. Finally, in every homogeneous region which is referred to by the subscript p,$p = u, l$:

$$\mathcal{F}_p(x^1,x^2) = \sum_{mq} F^+_{p,mq}A^+_{p,q}U_m(x^1)\exp(-i\beta_{p,q}(x^2-x_p^2))+ \sum_{mq} F^-_{p,mq}A^-_{p,q}U_m(x^1)\exp(i\beta_{p,q}(x^2-x_p^2)) \tag{23}$$

$$\mathcal{G}_p(x^1,x^2) = \sum_{mq} G^+_{p,mq}A^+_{p,q}U_m(x^1)\exp(-i\beta_{p,q}(x^2-x_p^2))+ \sum_{mq} G^-_{p,mq}A^-_{p,q}U_m(x^1)\exp(i\beta_{p,q}(x^2-x_p^2)) \tag{24}$$

Fig.2 illustrates the vertical domain decomposition. Our goal is to determine the S matrix which links the complex amplitude of the modes on each side of the grating and which we define as:

$$\begin{bmatrix} A_u^+ \\ A_l^- \end{bmatrix} = [S] \begin{bmatrix} A_u^- \\ A_l^+ \end{bmatrix} \tag{25}$$

The introduction of S matrices allows to deal with any multi-layer structures in which all the layers share the same periodicity and whose borders are described by the same coordinate system. In that way, the present method can easily be hybridized with the FMM.

ii. In the grating region

ii.1 Pseudo spectral approach

In this approach, the function $V(x^2)$ is approximated by the of a set of suitable Lagrange-interpolating functions C_n and unknown grid point values $V(x_n^2)$ at collocation points x_n^2 as follows:

$$V(x^2) = \sum_n C_n(x^2)V(x_n^2) \tag{26}$$

Considering Tchebycheff polynomials T_n and Gauss-Lobatto points x_n^2 as basis functions and collocation points respectively, the explicit form of C_n is:

$$C_n(v(x^2)) = \frac{2}{N\sigma_n}\sum_{m=0}^{N}\frac{1}{\sigma_m}T_m(v_n)T_m(v(x^2)) \tag{27}$$

with $\sigma_0 = \sigma_N$ and $\sigma_n = 1$ for $1 \leq n \leq N-1$. Function $v(x^2)$ maps the physical domain $[x_l^2, x_u^2]$ onto the interval $[-1,1]$ where Tchebycheff polynomials are defined:

$$v(x^2) = 2\frac{x^2 - x_l^2}{x_u^2 - x_l^2} - 1 \tag{28}$$

On the interval $[-1,1]$, the grid points are

$$v_n = \cos\left(\frac{\pi n}{N}\right), \quad n = 0\cdots,N \tag{29}$$

which corresponds to collocation points x_n^2 in the grating region:

$$x_n^2 = x_l^2 + \frac{x_u^2 - x_l^2}{2}(1+v_n) \tag{30}$$

The Tchebycheff pseudo spectral method approximates the first-order derivative by a differentiation matrix **D** Denoting by V_n' and V_n the values of the derivative of $V(x^2)$ with respect to x^2 and of $V(x_2)$ respectively at collocation points x_n^2 the differentiation matrix is such that:

$$\partial_2 \begin{bmatrix} V_0 \\ V_1 \\ \vdots \\ V_N \end{bmatrix} = \begin{bmatrix} V_0' \\ V_1' \\ \vdots \\ V_N' \end{bmatrix} = \mathbf{D} \begin{bmatrix} V_0 \\ V_1 \\ \vdots \\ V_N \end{bmatrix} \tag{31}$$

The entries of **D** are:

$$D_{ij} = \frac{2}{x_u^2 - x_l^2}\begin{cases} (1+2N^2)/6 & i=j=0 \\ -(1+2N^2)/6 & i=j=N \\ -0.5v_j/(1-v_j^2) & i=j; 0<j<N \\ (-1)^{i+j}\sigma_i/\sigma_j(v_i-v_j) & \end{cases} \tag{32}$$

Let us write down $\mathbf{D}$ as:

$$\begin{bmatrix} d_1 & \mathbf{d_2} & d_3 \\ \mathbf{d_4} & \mathbf{d_5} & \mathbf{d_6} \\ d_7 & \mathbf{d_8} & d_9 \end{bmatrix} \tag{33}$$

where d_1, d_3, d_7, d_9 are the four corner entries of $\mathbf{D}$, $\mathbf{d_2}, \mathbf{d_8}$ are row vectors of length N, $\mathbf{d_4}, \mathbf{d_6}$ are column vector of length N, finally $\mathbf{d_5}$ is a N by N matrix. Note that the differentiation matrix is given by buit-in matlab function *cheb*. So, finally, in the grating region the field is written as:

$$\begin{aligned} \mathcal{F}(x^1, x^2) &= \textstyle\sum_{mn} F_{mn} U_m(x^1) \otimes V(x_n^2) \\ \mathcal{G}(x^1, x^2)) &= \textstyle\sum_{mn} G_{mn} U_m(x^1) \otimes V(x_n^2) \end{aligned} \tag{34}$$

which means that F and G are sampled along x^2 and expanded onto another basis along x^1. As already mentioned, in the present study $U_m(x^1)$ are pseudo-periodic functions. Actually, since the variation of the field along x^2 is sampled at the Gauss-Lobatto points, we have as many operators depending on x^1 as we have collocation points along x^2:

$$\partial_2 \begin{bmatrix} \mathcal{F}(x^1, x_n^2) \\ \mathcal{G}(x^1, x_n^2) \end{bmatrix} = \begin{bmatrix} \mathcal{L}_{11}(x^1, x_n^2) & \mathcal{L}_{12}(x^1, x_n^2) \\ \mathcal{L}_{21}(x^1, x_n^2) & \mathcal{L}_{21}(x^1, x_n^2) \end{bmatrix} \begin{bmatrix} \mathcal{F}(x^1, x_n^2) \\ \mathcal{G}(x^1, x_n^2) \end{bmatrix} \tag{35}$$

ii.2 Matrix operator

We are now ready to transform Eq(35) into a matrix equation. Firstly a matrix $[\mathbf{L}]_n$, $n = 0, 1, \cdots, N-1$ is associated to each $\mathcal{L}(x^1, x_n^2)$ by using the Galerkin method with the U_m as basis and test functions. Then, it is possible to associate in (x^1, x^2) space a matrix to operators ∂_2 and $\mathcal{L}(x^1, x^2)$.

$$\partial_2 \longrightarrow \mathbf{D} \otimes \mathbf{I} \tag{36}$$

where $\otimes$ denotes the Kronecker product and $\mathbf{I}$ the identity matrix.

$$\begin{bmatrix} \mathcal{L}_{11} & \mathcal{L}_{12} \\ \mathcal{L}_{21} & \mathcal{L}_{22} \end{bmatrix} \longrightarrow \begin{bmatrix} \mathbf{L_{11}} & \mathbf{L_{12}} \\ \mathbf{L_{21}} & \mathbf{L_{22}} \end{bmatrix} \tag{37}$$

$\mathbf{L_{pq}}$ are block diagonal matrices such that:

$$\mathbf{L_{pq}} = diag([\mathbf{L_{pq}}]_n)\ n \in 0, 1, \cdots, N-1\ p, q = 12 \tag{38}$$

that is:

$$\mathbf{L_{pq}} = \begin{bmatrix} [\mathbf{L_{pq}}]_{N-1} & \mathbf{0} & \mathbf{0} & \mathbf{0} & \mathbf{0} \\ \mathbf{0} & [\mathbf{L_{pq}}]_{N-2} & \mathbf{0} & \mathbf{0} & \mathbf{0} \\ \mathbf{0} & \mathbf{0} & \ddots & \mathbf{0} & \mathbf{0} \\ \mathbf{0} & \mathbf{0} & \mathbf{0} & [\mathbf{L_{pq}}]_1 & \mathbf{0} \\ \mathbf{0} & \mathbf{0} & \mathbf{0} & \mathbf{0} & [\mathbf{L_{pq}}]_O \end{bmatrix} \tag{39}$$

Since the chosen $U_m(x^1)$ are complex exponentials, the derivation of the coefficients of matrices $[\mathbf{L}_{pq}]$ follows the rules of any Fourier based methods. Let us introduce $\mathbf{F}$ and $\mathbf{G}$ the column vectors formed by the concatenation of the F_{mn} and the G_{mn} respectively:

$$\begin{aligned} \mathbf{F} &= [\mathbf{F}_{N-1}, \mathbf{F}_{N-2}, \cdots, \mathbf{F}_1, \mathbf{F}_0]^T \\ \mathbf{G} &= [\mathbf{G}_{N-1}, \mathbf{G}_{N-2}, \cdots, \mathbf{G}_1, \mathbf{G}_0]^T \end{aligned}$$

and let us denote $\overline{\overline{\mathbf{F}}}$ and $\overline{\overline{\mathbf{G}}}$ the restriction of the above vectors to the $N-2$ interior points

$$\overline{\overline{\mathbf{F}}} = [\mathbf{F}_{N-2}, \cdots, \mathbf{F}_1,]^T$$

$$\overline{\overline{\mathbf{G}}} = [\mathbf{G}_{N-2}, \cdots, \mathbf{G}_1]^T$$

The matrix form of Eq.(35) writes:

$$\begin{bmatrix} \mathbf{D} \otimes \mathbf{I} & \cdots \\ \cdots & \mathbf{D} \otimes \mathbf{I} \end{bmatrix} \begin{bmatrix} \mathbf{F} \\ \mathbf{G} \end{bmatrix} = \begin{bmatrix} \mathbf{L_{11}} & \mathbf{L_{12}} \\ \mathbf{L_{21}} & \mathbf{L_{22}} \end{bmatrix} \begin{bmatrix} \mathbf{F} \\ \mathbf{G} \end{bmatrix} \tag{40}$$

Eq(40) is a matrix equation of the size $N \times M$. The N parameter is more or less equivalent to the number of layers in the MMFE.

At the end points of the inhomogeneous region x_0^2 and x_{N-1}^2 the tangential components of the field are represented by vectors $\mathbf{F}_0$ $\mathbf{G}_0$ (output) and $\mathbf{F}_{N-1}$ $\mathbf{G}_{N-1}$ (input). They also correspond to modal expansions of the field in the homogeneous upper and lower regions. It is seen that the size of the matrix necessary to solve the problem is $N \times M$. Using Gauss elimination as such to solve the problem makes the complexity of the algorithm $O((N \times M)^3)$. The latter could be significantly diminished by using iterative algorithms.

iii. Matching field expansion at the border of the three regions

The remaining task is to match the transverse components of the field at the upper and lower face of the grating in order to compute the modal coefficients of

the reflected and transmitted waves. At the upper face $x^2 = x_u^2$, we have:

$$\mathcal{F}(x^1, x_u^2) = \mathcal{F}_u(x^1, x_u^2) \;\; \mathcal{G}(x^1, x_u^2) = \mathcal{G}_u(x^1, x_u^2) \quad (41)$$

and at the lower one $x^2 = x_l^2$, we have:

$$\mathcal{F}(x^1, x_l^2) = \mathcal{F}_u(x^1, x_l^2) \;\; \mathcal{G}(x^1, x_l^2) = \mathcal{G}_u(x^1, x_l^2) \quad (42)$$

When projected onto the basis of U_m functions the above relations have the matrix form:

$$\begin{array}{l} \mathbf{F}_{N-1} = \mathbf{F}_u^+ \mathbf{A}_u^+ + \mathbf{F}_u^+ \mathbf{A}_u^- \\ \mathbf{G}_{N-1} = \mathbf{G}_u^+ \mathbf{A}_u^+ + \mathbf{G}_u^- \mathbf{A}_u^- \\ \mathbf{F}_0 = \mathbf{F}_l^+ \mathbf{A}_l^+ + \mathbf{F}_l^- \mathbf{A}_l^- \\ \mathbf{G}_0 = \mathbf{G}_l^+ \mathbf{A}_l^+ + \mathbf{G}_l^- \mathbf{A}_l^- \end{array} \quad (43)$$

According to Eq(40) we have an homogeneous system with $2 \times N \times M$ unknonws and equations. In this system $4 \times M$ lines correspond to the upper and lower faces of the grating. For $\mathbf{F}$, these lines are:

$$d_1 \mathbf{F}_{N-1} + [\mathbf{d}_2 \otimes \mathbf{I}]\, \overline{\overline{\mathbf{F}}} + d_3 \mathbf{F}_0 = [\mathbf{L_{11}}]_{N-1} \mathbf{F}_{N-1} + [\mathbf{L_{12}}]_{N-1} \mathbf{G}_{N-1} \quad (44)$$

$$d_7 \mathbf{F}_{N-1} + [\mathbf{d}_8 \otimes \mathbf{I}]\, \overline{\overline{\mathbf{F}}} + d_9 \mathbf{F}_0 = [\mathbf{L_{11}}]_0 \mathbf{F}_0 + [\mathbf{L_{12}}]_0 \mathbf{G}_0 \quad (45)$$

In the above lines, we substitute $\mathbf{F}_{N-1}$ and $\mathbf{F}_0$ with their expressions in terms of the modal amplitudes of the field in the homogeneous regions. Moreover, we do not take into account the lines corresponding to $\mathbf{G}_{N-1}$ and $\mathbf{G}_0$. Hence, finally, the system to be solved is now of size $2 \times (N-1) \times M$. It writes :

$$\begin{bmatrix} \mathbf{Z_5} & \mathbf{0} & \mathbf{Z_4^+} & \mathbf{Z_6^-} \\ \mathbf{0} & \mathbf{Y_5} & \mathbf{Y_4^+} & \mathbf{Y_6^-} \\ \mathbf{Z_2} & \mathbf{0} & \mathbf{Z_1^+} & \mathbf{Z_3^-} \\ \mathbf{Z_8} & \mathbf{0} & \mathbf{Z_7^+} & \mathbf{Z_9^-} \end{bmatrix} \begin{bmatrix} \overline{\overline{\mathbf{F}}} \\ \overline{\overline{\mathbf{G}}} \\ \mathbf{A}_u^+ \\ \mathbf{A}_l^- \end{bmatrix} = \begin{bmatrix} \mathbf{Z_4^-} & \mathbf{Z_6^+} \\ \mathbf{Y_4^-} & \mathbf{Y_6^+} \\ \mathbf{Z_1^-} & \mathbf{Z_3^+} \\ \mathbf{Z_7^-} & \mathbf{Z_9^+} \end{bmatrix} \begin{bmatrix} \mathbf{A}_u^- \\ \mathbf{A}_l^+ \end{bmatrix} \quad (46)$$

$$\begin{bmatrix} \mathbf{Z_5} & \mathbf{0} \\ \mathbf{0} & \mathbf{Y_5} \end{bmatrix} = \begin{bmatrix} \mathbf{d_5} \otimes \mathbf{I} & \mathbf{0} \\ \mathbf{0} & \mathbf{d_5} \otimes \mathbf{I} \end{bmatrix} - \overline{\overline{\mathbf{L}}} \quad (47)$$

$$\mathbf{Z_2} = \mathbf{d_2} \otimes \mathbf{I} \quad (48)$$

$$\mathbf{Z_8} = \mathbf{d_8} \otimes \mathbf{I} \quad (49)$$

$$\mathbf{Z_4^\pm} = \mathbf{d_4} \otimes \mathbf{F}^{\pm(1)} \quad (50)$$

$$\mathbf{Z_6^\pm} = \mathbf{d_6} \otimes \mathbf{F}^{\pm(3)} \quad (51)$$

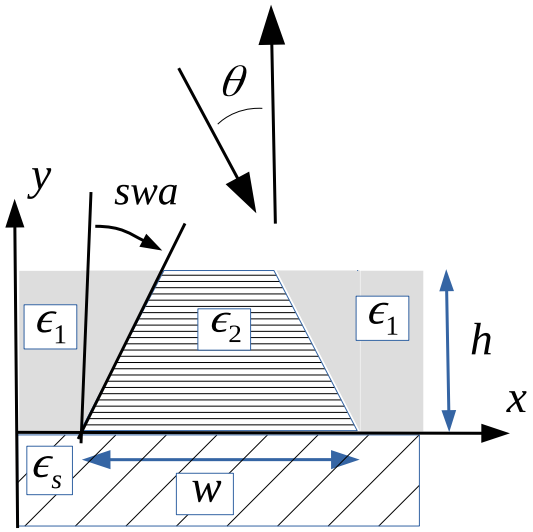

Figure 3: *Illustration of a trapezoidal grating*

$$\mathbf{Y_4^\pm} = \mathbf{d_4} \otimes \mathbf{G}^{\pm(1)} \quad (52)$$

$$\mathbf{Y_6^\pm} = \mathbf{d_6} \otimes \mathbf{G}^{\pm(3)} \quad (53)$$

$$\begin{array}{l} \mathbf{Z_1^+} = (d_1 \mathbf{I} - [\mathbf{L_{11}}]_{N-1})\, \mathbf{F}^{+(1)} - [\mathbf{L_{12}}]_{N-1} \mathbf{G}^{+(1)} \\ \mathbf{Z_1^-} = (-d_1 \mathbf{I} + [\mathbf{L_{11}}]_{N-1})\, \mathbf{F}^{-(1)} + [\mathbf{L_{12}}]_{N-1} \mathbf{G}^{-(1)} \\ \mathbf{Z_3^-} = d_3 \mathbf{F}^{-(3)} \\ \mathbf{Z_3^+} = -d_3 \mathbf{F}^{+(3)} \end{array} \quad (54)$$

$$\begin{array}{l} \mathbf{Z_9^+} = (-d_9 \mathbf{I} + [\mathbf{L_{11}}]_0)\, \mathbf{F}^{+(3)} + [\mathbf{L_{12}}]_0 \mathbf{G}^{+(3)} \\ \mathbf{Z_9^-} = (d_9 \mathbf{I} - [\mathbf{L_{11}}]_0)\, \mathbf{F}^{-(3)} - [\mathbf{L_{12}}]_0 \mathbf{G}^{-(3)} \\ \mathbf{Z_7^+} = d_7 \mathbf{F}^{+(1)} \\ \mathbf{Z_7^-} = -d_7 \mathbf{F}^{-(1)} \end{array} \quad (55)$$

It is seen that the solution of the system Eq46 gives simultaneously the sought S matrix and the field at the collocation points.

IV. Results

i. Comparison with published data

In this section, we validate our code by comparing our results with already published data obtained with C-method combined with adaptive spatial resolution [7]. The first examples are for trapezoidal gratings illustrated on Fig.3 and whose parameters are: $h = 1$, $d = 1$, $w = .65$, $sidewallangle(swa) = .005$ rad, $\varepsilon_1 = 1$, $\theta = \pi/4$, $\lambda = 1$. We consider both a dielectric grating with $\varepsilon_2 = \varepsilon_s = 1.5^2$, and a metallic grating with

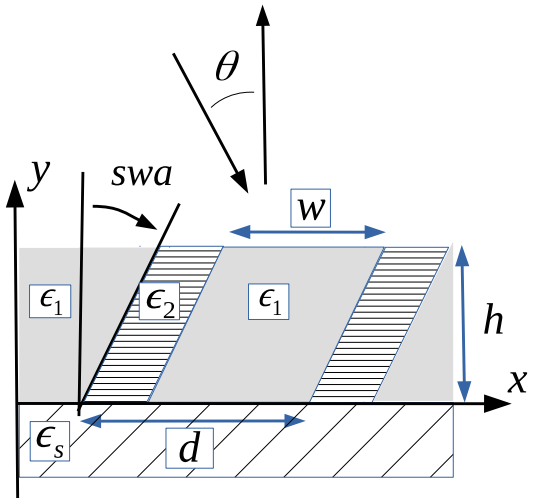

Figure 4: *Illustraion of a slanted grating*

$\varepsilon_2 = \varepsilon_s = (0.3 - i7)^2$ respectively. ε_s designates the permittivity of the substrate. The truncation parameters for the Matched Coordinates Method are $M = 40$, $N = 20$ and the adaptive spatial resolution parameter η is set to one. Efficiences are reported in table1 and table 2 respectively. It is seen that both methods are in very good accordance.

	TE polarisation		TM polarisation	
	ASR-C	MCM	ASR-C	MCM
R_{-3}	0.0060	0.0060	0.0067	0.0067
R_{-2}	0.009	0.009	0.0004	0.004
R_{-1}	0.0016	0.0016	0.0003	0.0003
R_0	0.055	0.055	0.0071	0.0071
T_{-4}	0.0835	0.0835	0.045	0.045
T_{-2}	0.5223	0.5224	0.3770	0.3769
T_{-1}	0.1319	0.1319	0.2122	0.2122
T_0	0.1148	0.1147	0.2222	0.2222
T_1	0.0045	0.0045	0.0841	0.0842
T_2	0.0790	0.0791	0.0451	0.0450

Table 1: *Efficiencies of a dielectric trapezoidal grating (ASR-C = C-Method with adaptive resolution, MCM = Matched Coordinate Method)*

A second class of gratings concerns dielectric or metallic slanted gratings represented on Fig.4. The parameters are: $h = .2$, $d = 1$, $w = .5$, $swa = 10°$, $\varepsilon_1 = 1.5^2$ (dielectric case)or $\varepsilon_1 = (.22 - i6.71)^2$ (metallic case), $\varepsilon_2 = 1$, $\varepsilon_s = 1.45^2$, $\theta = 30°$, $\lambda = 1$. The truncation parameters for the Matched Coordinates Method are $M = 16$, $N = 10$ and the adaptive spatial resolution parameter η is set to one. Here the reference

	TE polarisation		TM polarisation	
	ASR-C	MCM	ASR-C	MCM
R_{-3}	0.0092	0.0092	0.5054	0.5053
R_{-2}	0.0040	0.0040	0.0772	0.0773
R_{-1}	0.0718	0.0716	0.1484	0.1487
R_0	0.8870	0.8878	0.08630	0.0855

Table 2: *Reflected efficiences of a metallic trapezoidal grating.*

method is the polynomial modal method [13]. Results are tabulated in table3 for the dielectric case and in table 4 for the metallic case respectively. Once more, the comparison of the computed efficiencies with the two methods is more than satisfactory.

	TE polarisation		TM polarisation	
	PMM	MCM	PMM	MCM
R_{-1}	0.0179	0.0179	0.0231	0.0231
R_0	0.0137	0.0137	0.0011	0.0011
T_{-1}	0.0399	0.0399	0.0227	0.0227
T_0	0.9286	0.9286	0.9531	0.9531

Table 3: *Efficiencies of a slanted dielectric grating (PMM = Polynomial Modal Method)*

ii. Comparison of convergence with FMM

The FMM is very popular and versatile, but its simplicity comes from the approximation of the grating profile by a staircase profile. This approximation is all the more penalizing when the index contrast is high and the sides of the grating deviate from the vertical. In the case of a metallic grating, convergence is even impossible. In order to illustrate the improvement in term of convergence of MCM compared to FMM we consider the zeroth transmitted order of a dielectric trapezoidal grating with a sidewall angle $SWA = 20°$ deposited on a glass substrate with $\epsilon_s = 1.5^2$. The other parameters are: $\epsilon_1 = 1$, $\epsilon_2 = 3.5^2$, $\theta = 0$, $\lambda = .65$, $d = 1$, $w = 0.8640$. The reference values are obtained thanks to the ASR C-method with truncation

	TE polarisation		TM polarisation	
	PMM	MCM	PMM	MCM
R_{-1}	0.2358	0.2359	0.2245	0.2248
R_0	0.4268	0.4267	0.3113	0.3113
T_{-1}	0.1646	0.1646	0.2067	0.2066
T_0	0.1557	0.1557	0.2381	0.2381

Table 4: *Efficiencie of a slanted metallic grating*

order $M = 250$. We got $Te_0\text{ref} = 0.508523257$ and $Tm_0\text{ref} = 0.127159134$. We define an error function in the following way:

$$err = \log(|T\text{computed} - T\text{ref}|) \tag{56}$$

Convergence plots are shown in Fig6 and Fig7 for TE polarization and on Fig8 and Fig9 for TM polarization. Unquestionably, numerical convergence is faster with MCM than with FMM even in the case of TE polarization.

iii. Exemple of application

Lastly, in order to illustrate the possibilities of the new algorithm we investigate a grating designed for metrology applications, see Fig.5. In that grating, aluminum is deposited at the bottom and at the top of the grooves etched in fused silica which makes the grating a three layer stack. In the present implementation of our code, a S matrix is computed for each layer. The upper layer is a simple lamellar grating. Although we did not do it that way, its S matrix could be obtained with the Fourier Modal Method. Indeed, our method can be hybridized with the FMM every time local translation invariance makes it possible. Table5

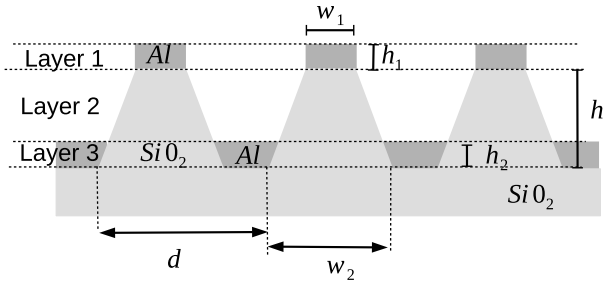

Figure 5: *Grating for metrology applications*

shows the specular and minus one reflected orders for a grating enlightened under normal incidence at $\lambda = 650\,nm$ for different groove depth. In every case, the thickness of aluminium is $100\,nm$, its optical index is $n = 1.488 - i7.821$. Fused silica optical index is $n = 1.456$. The parameters are $d = 20\,\mu m$, $w_1 = d/3$, $w_2 = 2d/3$. The vertical sampling parameter in layers 1, 2 and 3 is $N = 20$, $N = 26$, $N = 20$ respectively. The truncation number M is $M = 100$. For comparison purpose, we have also analysed that grating with the FMM and the same truncation parameters M and N (except in layer 1 where $N = 1$. Results are reported in Table 6. The discrepancy between FMM and MCM is observable but remains acceptable probably because

	TE polarisation		TM polarisation	
Depth	R_0	R_{-1}	R_0	R_{-1}
0.65	0.6662	0.0009	0.6721	0.0009
0.48	0.0205	0.3363	0.0195	0.3372
0.325	0.6991	0.0004	0.7090	0.0004
0.16	0.0047	0.3621	0.0036	0.3632

Table 5: *Efficiencies of a grating dedicated to metrology applications*

	FMM		MCM	
Depth	R_0	R_{-1}	R_0	R_{-1}
0.65	0.6669	0.0009	0.6721	0.0009
0.48	0.0201	0.3360	0.0195	0.3372
0.325	0.7059	0.0004	0.7090	0.0004
0.16	0.0004	0.3621	0.0036	0.3632

Table 6: *Comparison of efficiencies in TM polarization for a grating dedicated to metrology applications (FMM = Fourier Modal Method)*

on the one hand, the index contrast in layer 2 is rather small, and on the other hand, layer 1 and layer 3 which comprise metal are thin compared to the wavelength.

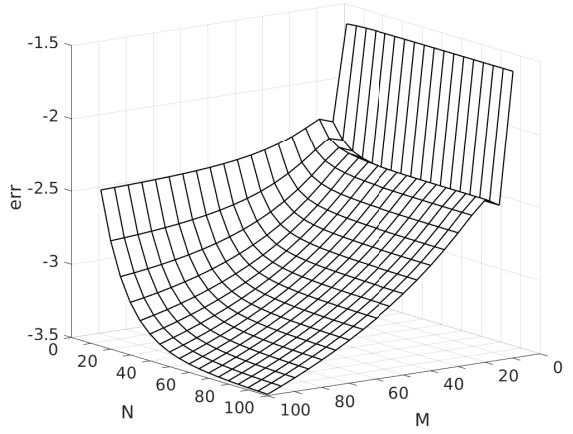

Figure 6: *Convergence of the zeroth TE transmission order computed with MMFE.*

V. Conclusion

In this paper, a formulation based on matched coordinates has been proposed. In this formulation, the coefficients of Maxwell's equations depend on the axial direction which makes impossible the solution

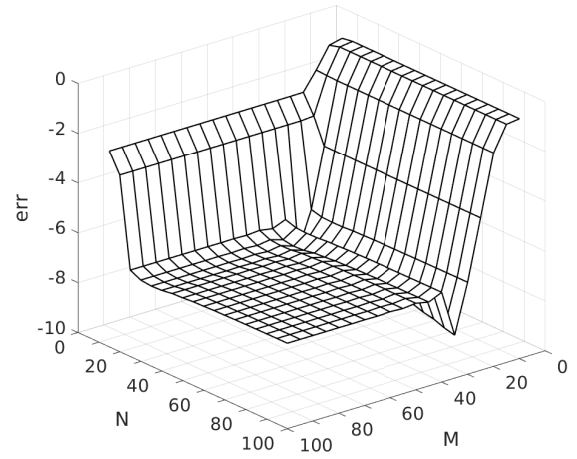

Figure 7: *Convergence of the zeroth TE transmission order computed with MCM.*

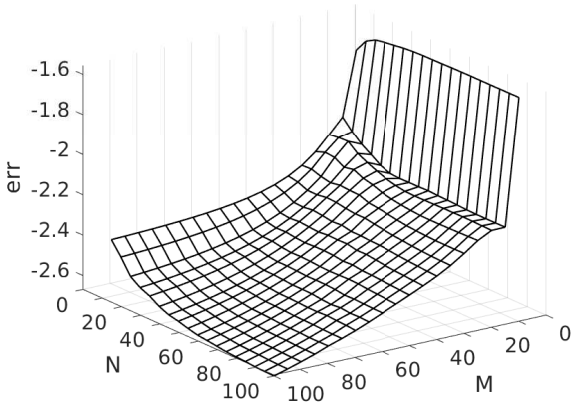

Figure 8: *Convergence of the zeroth TM transmission order computed with MMFE.*

of the problem with a modal technique. Instead a pseudo-spectral approach was implemented whereas a Fourier expansion along the transverse direction was kept on. Hence the hybridization with the Fourier Modal Method is straightforward. As all others methods, the matched coordinates method that we have just presented has its pros and its cons. However, its definitive advantage is that it does not introduce any approximation in the profile. Many improvements are now possible: for example the use of polynomial bases in the transverse direction or the iterative resolution of the final algebraic system.

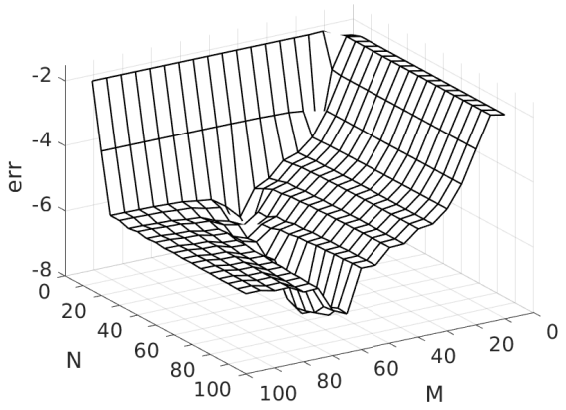

Figure 9: *Convergence of the zeroth TM transmission order computed with MCM.*

VI. Disclosures

The authors declare no conflict of interest.

References

[1] M. G. Moharam and T. K. Gaylord, "Diffraction analysis of dielectric surface-relief gratings," *J. Opt. Soc. Am A,*vol.72, p. 1385–1392 (1982).

[2] "Electromagnetic theory of gratings",(ed. R.Petit), Springer,(1980)

[3] "Gratings:Theory and Numeric Application", (ed. E.Popov), Institut Fresnel,AMU, CNRS.

[4] , J. Chandezon, D. Maystre, and G. Raoult, "A new theoretical method for diffraction gratings and its numerical application," J. Opt, vol. 11, pp.235–241 (1980).

[5] ,J. Chandezon, M.T. Dupuis, G. Cornet, and D. Maystre, "Multicoated gratings: a differential formalism applicable in the entire optical region," J. Opt. Soc. Am, vol.72, pp.839-846, (1982).

[6] G. Granet, 1999, "Reformulation of the lamellar grating problem through the concept of adaptive spatial resolution," *J. Opt. Soc. Am. A,* Vol.16, pp. 2510–2516 (1999).

[7] G.Granet, J.Chandezon, J.P Plumey, and K.Raniriharinosy, "Reformulation of the coordinate transformation method through the

concept of adaptive spatial resolution. Application to trapezoidal gratings,"*J. Opt. Soc. Am. A,* Vol.18, pp. 2102–9108 (2001).

[8] E.Popov and M.Neviere, "Grating theory: new equations in Fourier space leading to fast converging results for TM polarization," J.Opt.Soc. Am A, vol.17,p.1773–1784 (2000).

[9] A.Khavasi,A.K.Jahromi, and K.Mehrany, "Longitudinal Legendre Polynomial expansion of electromagnetic fields for analysis of arbitrary-shaped gratings," J.Opt.Soc. Am A, vol.25,p.1564–1573 (2008).

[10] C. J. Raymond, M.R. Murnane, S.Prins, S. Sohail, H. Naqvi, J. Mcneil, J. W. Hosch, "Multiparameter grating metrology using optical scatterometry", Journal of Vacuum Science and Technology, vol. 15, pp. 361-368, (1997).

[11] J.Bischoff, T.Pahl, P.Lehmann, E.Manske "Model Based Dimensional Optical Metrology" Proc. SPIE 11352-27 (2020).

[12] T.Pahl, S.Hagemeyer, M.Künne, D.Yang, P.Lehmann, "3D modeling of coherence scanning interferometry on 2D surfaces using FEM," *Optics Express,* Vol.28 pp.39807–39826 (2020)

[13] G.Granet, M.H.Randriamihaja, and K.Raniriharinosy, "Polynomial modal analysis of slanted lamellar gratings,"*J. Opt. Soc. Am. A,* Vol.34, pp. 975–982 (2017).